

# Crystallinity and Mechanical Properties of PP-Homopolymers as Influenced by Molecular Structure and Nucleation

MARKUS GAHLEITNER,<sup>1,\*</sup> JOHANNES WOLFSCHWENGER,<sup>1</sup> CLAUDIA BACHNER,<sup>2</sup> KLAUS BERNREITNER,<sup>1</sup> and WOLFGANG NEIBL<sup>1</sup>

<sup>1</sup>PCD Polymere GmbH, St. Peter Straße 25, A-4021 Linz, Austria; and <sup>2</sup>J. Kepler University Linz, Inst. of Chemistry, Altenbergerstr. 69, A-4040 Linz, Austria

## SYNOPSIS

The evolution of crystallinity and mechanical properties of two different series of PP-homopolymers (RE grades coming directly from the polymerization reactor and CR grades priorly subjected to a defined degradation process) as influenced by the molar mass and heterogeneous nucleation was investigated, including one highly isotactic material to check the tacticity influence. In principle, the effects seem explainable by differences in the number of nuclei and the spherulitic growth speed, which were determined separately. The nucleation effects are similar for all materials, but strongly dependent of the molar mass of the materials. Apart from the bulk material properties, also the development of shear-induced structures is strongly influenced by molar mass and nucleation, contributing additionally to mechanics. © 1996 John Wiley & Sons, Inc.

## INTRODUCTION

In recent years, polypropylene has been able to steadily increase its market share by entering new application segments. The reasons for a further continuation of this trend are a very advantageous price/property relation and, even more important, the possibility to modify this polymer to a wide range of final properties.<sup>1,2</sup> In the most simple case of PP-homopolymers, two factors apart from processing conditions influence the mechanical properties of the product: rheological behavior and solidification—or crystallization—behavior, respectively. Both factors are, in turn, determined by the molecular structure, for instance, the chain structure or stereoregularity and the chain length or molar mass distribution (MMD).

In the course of tailor-made material development, these correlations become increasingly important. A look at the respective literature, however, reveals that such influences have so far rather been

studied for the rheology<sup>3–6</sup>—than for the crystallization-side<sup>7–9</sup> of the problem. The effect of the difference between reactor grades (RE-PP) and peroxide-degraded grades (“controlled rheology” or CR-PP) on the rheological behavior can, for example, be easily explained by the narrow MMD of the latter, but the differences in the mechanical properties of these materials, which are already equally well known for quite some time, have so far been missing a satisfactory explanation.

In industrial practice, final properties of PP are often further adjusted through the addition of nucleating agents.<sup>10</sup> One takes advantage here of the slow course of solidification in polymers, which leads to a separation of the nucleation and the spherulitic growth process. Figure 1 (adapted from ref. 11) gives an impression of this effect, which allows influencing of the final crystallinity to a large extent. As homogeneous nucleation has its maximum at lower temperatures than crystallite growth, the additional heterogeneous nucleation allows taking advantage of higher crystallization velocities, thus arriving at a higher overall crystallinity and a finer morphology on the spherulitic level. Here, again, theoretical models are lacking; it is especially unclear which

\* To whom correspondence should be addressed.

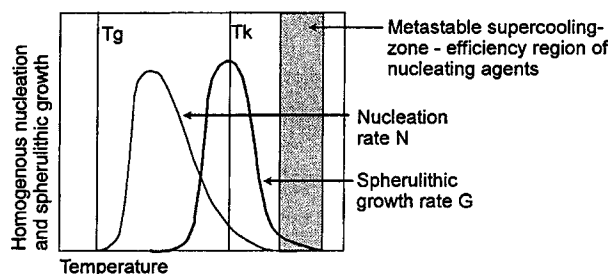


**Figure 1** Separation of nucleation and crystallite growth in the crystallization of polymers (adapted from ref. 9); effective region of heterogeneous nucleating agents.

structural factors cause the nucleating effect of a certain substance.

Additionally, the correlations found in practice are even more complex than expected. The stiffness (or flexural modulus) of a material is influenced by the degree of crystallinity as well as the transparency (or light scatter). The application of various nucleating agents, however, leads to different effects on both quantities (see Fig. 2). Thereby, a classification of the technically used nucleating agents into (a) standard types (like talc, sodium benzoate, etc.), (b) clarifying types (e.g., special derivatives of sorbit), and (c) reinforcing types (e.g., special organophosphates) can be made. Special effects can finally be induced by nucleating agents, which favor a special crystal modification ( $\beta$  or  $\gamma$ ).<sup>12</sup>

The primary scope of the investigations presented here was to find quantitative correlations as well as theoretical explanations for the influence of molecular structure (stereoregularity, MMD, difference RE-/CR-PP) on one hand and nucleation on the other hand on the mechanical properties. Various sources<sup>7,13,14</sup> present the effect of a stiffness increase with falling molar mass (e.g., weight average molar mass,  $M_w$ ) in case of RE-PP and a stiffness decrease with falling  $M_w$  in case of CR-PP. If classical concepts of polymer crystallization<sup>7,11</sup> are taken into account, only the first of these two effects seem explicable: shorter polymer chains should be preferred in the formation of lamellae and crystallites by their higher mobility and ability to fold. Why this effect does not appear with CR-PP, or is, moreover, even reversed, is not obvious at first sight.

Only a few articles have been published so far concerning the effects of stereoregularity on mechanical properties,<sup>15-18</sup> even if there are several patents claiming mechanical advantages, for instance, higher crystallinity and stiffness, for highly isotactic PP grades.<sup>19</sup> In our case, only one experimental material was included to complete the investigation.

## Materials and Investigations

Two series of PP-homopolymers were produced: (a) RE-PP grades in a pilot plant (propylene-bulk, Spheripol-process, commercial fourth-generation Ziegler/Natta catalyst) with variation of the MFR (ISO 1133, 230°C/2.16 kg) between 0.4 and 150 g/10 min ( $H_2$ -regulation); one additional material with higher isotacticity was also produced at MFR = 8.4 g/10 min by properly adjusting the catalyst system (HI-RE-PP); (b) CR-PP grades based on the RE-grade with highest  $M_w$  by peroxide-controlled degradation in a twin-screw extruder with variation of MFR between 3.4 and 149 g/10 min.

The fact that these materials were separately produced in a rather cost-intensive way secured a homogeneous basic structure of all materials, for example, regarding the shape of MMD and chain tacticity. In detail, the stereoregularity (isotactic pentads content) was checked using  $^{13}\text{C}$ -NMR according to a method developed by Zambelli<sup>20</sup> for all materials with MFR  $\approx$  8 g/10 min; respective data are included in Table II. To determine the effect of nucleation, 0.1 wt % of a nucleating agent was added in a second extrusion step, which did not significantly change the molar mass of the samples.

The MMD data of all materials (summarized in Table I) were determined on a Waters 150C GPC at 135°C in trichlorobenzene; it turned out that they correlated very well to the MFR measurements (see Fig. 3). Crystallinity was investigated via DSC (according to DIN 53765) on a TA Instruments DSC 512C using a heat/cool/heat cycle between +23 and +250°C at rates of 10 K/min. As the melting enthalpy represents only an indirect determination of crystallinity,<sup>21</sup> the density of the three MFR 8 grades (RE, HI-RE, and CR) was determined on original samples additionally. As outlined in Table II, the data correlate quite well, even if the absolute levels are different, confirming the relativity of the DSC method. Mechanical properties were measured in flexural testing (DIN 53452/57) and flexural impact (ISO 179 1eA, Charpy V-notch) at +23°C on injection-molded samples (dimension 80 × 10 × 4 mm; injection according to DIN 16774). The internal structure of these samples was investigated using light microscopy on cross-sections perpendicular to the direction of injection.

Special investigations were carried out to separate the effects of nucleation and spherulitic growth. Similar to earlier investigations,<sup>22</sup> both factors were determined on the RE, HI-RE, and CR grades at MFR = 8 g/10 min. In contrast to the previous work, where the growth rate had been determined from

front growth measurements of a transcrystalline layer in a slab-like sample<sup>23</sup> and the number of nuclei from a DSC experiment,<sup>24</sup> a more direct approach was used here in both cases.

The spherulitic growth rate was measured using thin film crystallization, a method that had been developed in the working group of Janeschitz-Kriegl.<sup>25</sup> Here, a thin material sample is molten between two glass slides, subsequently kept at a temperature  $T_c$  below the thermodynamic melting point ( $T_m$ ) for a defined time  $t_c$ , and then quenched in ice water. Using a light microscope, the size of the spherulites having formed during  $t_c$  is measured and the growth speed  $G$  can then be determined from a plot of spherulite radius vs. crystallization time. To ensure correct calculation, the largest spherulite formed has to be evaluated. For the present investigation,  $T_c$  was varied in the range between 82 and 122°C.

To determine the number of nuclei at a certain  $T_c$ , DSC experiments were carried out at different cooling rates. The actual value of  $T_c$  was calculated from the DSC plots as described in ref. 24, taking into account the heat transfer problems. From the solidified DSC samples microtome cuts were taken that were then microphotographed. By counting the number of spherulites in a certain area, the area density  $N_A$  can be determined, from which the vol-

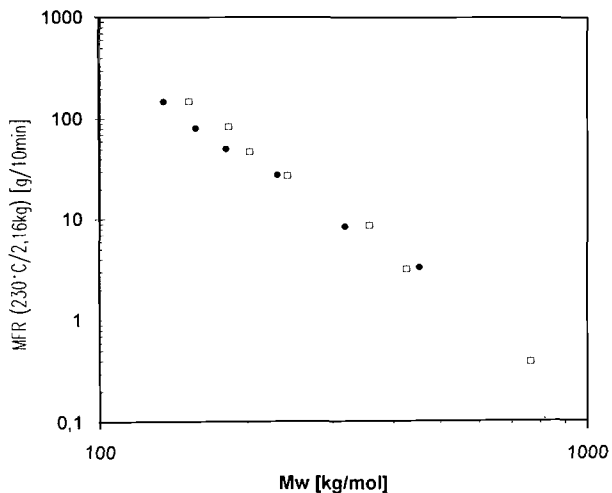


**Figure 3** Correlation between weight average molar mass and MFR (230°C/2.16 kg) for RE (□) and CR types (●).

ume density  $N_V$  is then calculated using the simple approximation

$$N_V[m^{-3}] = N_A[m^{-2}]^{3/2} \quad (1)$$

By varying the cooling rate between 10 and 50 K min<sup>-1</sup>, the  $T_c$  range between 106 and 117°C could be covered.

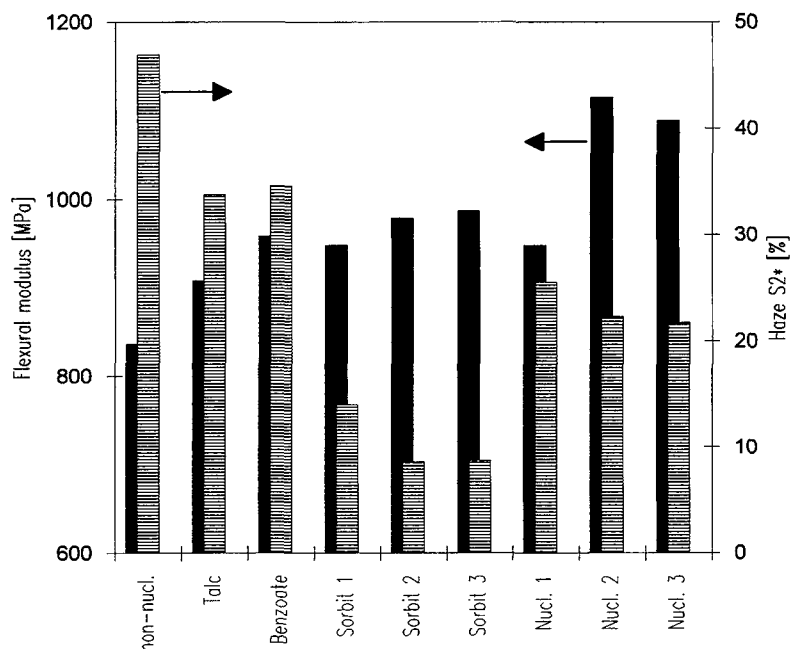


**Figure 2** Effect of different nucleating agents (standard types: Na-Benzooate, Talc; clarifiers: sorbit 1-3; reinforcing types: Nucl. 1-3) on stiffness (flexural modulus measured as described in chapter 2) and transparency (measured on injection molded plaques of 2 mm thickness).

**Table I** MMD-Data (from GPC) and MFR (230°C/2, 16 kg) for All Investigated Materials

Base Mat. No.	Nucl. Mat. No.	Type (RE/CR)	$M_w$ [kg/mol]	$M_n$ [kg/mol]	$M_w/M_n$ [-]	MFR [g/10 min]
5964/01	5973/01	RE	766	138	5.5	0.4
5964/02	5973/02	RE	426	78	5.5	3.2
5964/03	5973/03	RE	357	71	5	8.6
5964/04	5973/04	RE	242	49	4.5	27.5
5964/05	5973/05	RE	203	42	4.9	47.3
5964/06	5973/06	RE	183	31	5.9	83.7
5964/07	5973/07	RE	152	23	6.5	150.3
7606/01	8699/12	HI-RE	384	75	5.1	8.4
5964/08	5973/08	CR	453	123	3.5	3.4
5964/09	5973/09	CR	318	102	3.1	8.6
5964/10	5973/10	CR	231	83	2.8	28
5964/11	5973/11	CR	181	59	2.7	51
5964/12	5973/12	CR	157	59	2.7	81
5964/13	5973/13	CR	135	55	2.5	149

## RESULTS AND DISCUSSION

### Influence of Molecular Structure

As to be expected from the introductory remarks, the DSC scans showed increasing crystallinity with decreasing  $M_w$  or increasing MFR, respectively, expressed in Figure 4 by the crystallization enthalpy  $H_C$ . The increase, however, is significantly less pronounced in case of the CR grades. Taking into account the theoretical value of the melting enthalpy  $H_M$  for a "fully crystalline" PP, 209 J/g,<sup>26</sup> the relative crystallinity of the samples was in the region of 40–60%. Density measurements of injection-molded samples (cross-sections used) gave the same tendency in results (see Table II).

If the interest is shifted to mechanical properties, the flexural modulus ( $E_F$ ) exhibits the well-known picture of proportionality to  $\log$  (MFR) for the RE grades as well as a stagnation or even decrease for the CR grades (see Fig. 5). The effects were, however, less pronounced than in earlier investigations based on products from a hexane-slurry process.<sup>22</sup>

The notched impact strength ( $a_N$ ) of the materials decreases steadily with rising MFR in both series (RE and CR); at comparable MFR,  $a_N$  is always higher for the CR than for the RE grade (see Fig. 6). Here, again, a similar result was reached in the previous study,<sup>22</sup> where, however, a much narrower range of molecular weight had been covered. Generally, the reduction of  $a_N$  with falling molar mass is well known from the more simple case of glassy polymers like PS,<sup>27</sup> while the stiffness remains constant there. The impact effect there goes along with differences in the structure of the fracture surface

and is mainly attributed to entanglement effects, which are less pronounced at lower molar masses.

For semicrystalline polymers, the differences in mechanical properties have so far been mainly explained based on morphological differences,<sup>28</sup> more precisely, the spherulite size.<sup>29</sup> These are in turn closely connected to the two parameters  $G$  (spherulitic growth speed) and  $N_V$  (number of nuclei per unit volume) determined in the crystallization experiments. To avoid molar mass influences (which may be part of a later study), one RE and one CR grade each with comparable  $M_w$  and MFR were chosen for these measurements, complemented by the HI-RE grade. It appears that the differences in the crystallization behavior are mainly determined by the number of nuclei (see Fig. 7), where—rather independent of  $T_c$ —a difference of more than one decade between RE and CR grade can be observed. The values for the HI-RE material are between these extrema, but closer to the RE grade.

A different picture is obtained considering the chain regularity of the polymer, which is often connected to the crystallinity in the patent literature,<sup>19</sup> as an influence factor. There is evidence in the literature<sup>15–17,30</sup> for a strong influence on the spherulitic growth speed, which was, in principle, confirmed in our measurements (see Fig. 8). The tacticity range covered was significantly narrower for technical reasons, for instance, because the HI-RE material under investigation was part of a development program to increase the modulus. It appears that a significant effect on the spherulitic growth speed ( $G$ ) can be determined only between the RE and the HI-RE material, while all other parameters

**Table II Effect of Chain Regularity (mol %  $\langle$ mmmm $\rangle$ -Pentades According to Zambelli  $\langle I \rangle$ ) on Spherulitic Growth Speed, Crystallinity ( $c_D$  – rel. Crystallinity from Density,  $c_H$  – rel. Crystallinity from Melting Enthalpy) and Mechanics in Nonnucleated Form for RE-Type 5964/03, HI-RE-Type 7606/01, and CR-type 5964/09 (MFR 8)**

	RE Type	HI-RE Type	CR Type
$\langle$ mmmm $\rangle$ [mol %]	94.5	97.2	95.8
$G$ (102°C) [m/s]	$4.15 \cdot 10^{-6}$	$6.2 \cdot 10^{-6}$	$4.5 \cdot 10^{-6}$
$c_D$ , nonnucl. [%]	60.5	62.3	57.2
$c_H$ , nonnucl. [%]	52.7	56.4	52.2
$E_F$ (+23°C) [MPa]	1600	1750	1213
$a_N$ (+23°C) [kJ/m <sup>2</sup> ]	3.4	3.3	3.9

reflecting overall crystallinity (see Table II) are varying for all grades in the direction CR < RE < HI-RE. The actual values measured for  $G$  were about one decade above the data published by Cheng et al.,<sup>15-17</sup> which can most probably be attributed to a methodic problem in his case.<sup>25</sup>

Summarizing, these results allow a qualitative explanation of the effect seen in crystallinity at least. Furthermore, if a certain correlation between the degree of crystallinity and the stiffness is assumed,<sup>31</sup> the mechanical effects can be understood as well. However, prior investigations<sup>18,32</sup> also show that the processing conditions influence the final mechanics at least as strong as molecular factors. Even if all materials are processed in the same way (according to standard), this does not ensure the same conditions for crystallization for materials with different  $N_V(T_c)$  and  $G(T_c)$  dependencies. This applies, even stronger, to nucleated materials!

### Influence of Nucleation

The addition of a (heterogeneous) nucleating agent is seen in the primary DSC characterization in two effects: increase in the enthalpy of melting and crystallization ( $H_M$  and  $H_C$ , respectively), and increase in the apparent crystallization temperature ( $T_{c,app}$ ; the peak temperature of the crystallization exotherm is taken here to avoid complex calculations). The latter effect is often used in industrial practice to judge the effectiveness of nucleating agents,<sup>33,34</sup> as the relative changes observed are more significant than for the enthalpies. In case of comparative measurements on one polymer type (and keeping sample mass and geometry constant), this method seems acceptable, although from a theoretical point of view the evaluation of crystallization plots from the DSC

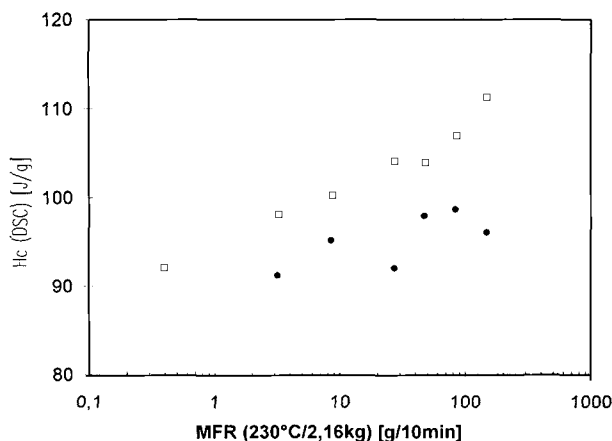


**Figure 4** Correlation between MFR (230°C/2.16 kg) and crystallization enthalpy ( $H_c$ ) for RE (□) and CR types (●).

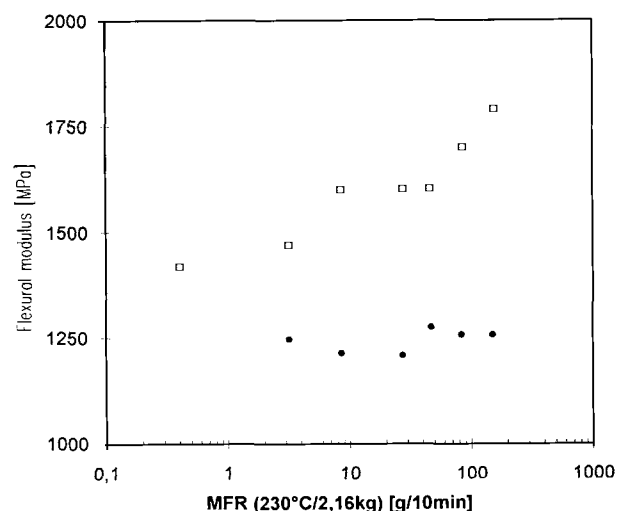


**Figure 5** Correlation between MFR (230°C/2.16 kg) and stiffness (flexural modulus,  $E_F$ ) for RE (□) and CR types (●).

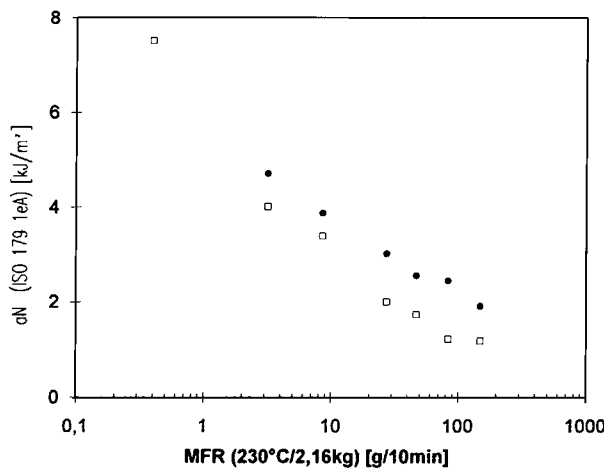


**Figure 6** Correlation between MFR (230°C/2.16 kg) and impact strength (ISO 179 1eA +23°C,  $a_N$ ) for RE (□) and CR types (●).

can only be carried out including corrections for the heat transfer in the instrument and measuring cell.<sup>24</sup>

The nucleation effects for the RE grades in the present series are presented in Figure 9. The variation in the difference between the crystallization temperature of the nucleated ( $T_{c,n}$ ) and the non-nucleated ( $T_{c,u}$ ) samples with rising MFR shows that the nucleation effect increases first and then decreases again with falling molar mass. For the high-isotacticity (HI-RE) grade, the basic value of  $T_c$  as well as the nucleation difference is in the same range as for the RE grade with the same MFR.

An analogous plot for the CR grades gives a different picture, namely, a rather constant difference of

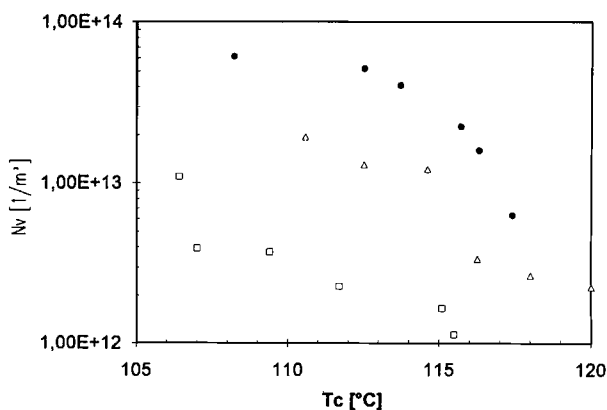


**Figure 7** Number of nuclei per unit volume as calculated from optical investigation of DSC samples crystallized at different cooling rates for RE-type 5964/03 (□), HI-RE-type 7606/01 (△), and CR-type 5964/09 (●).

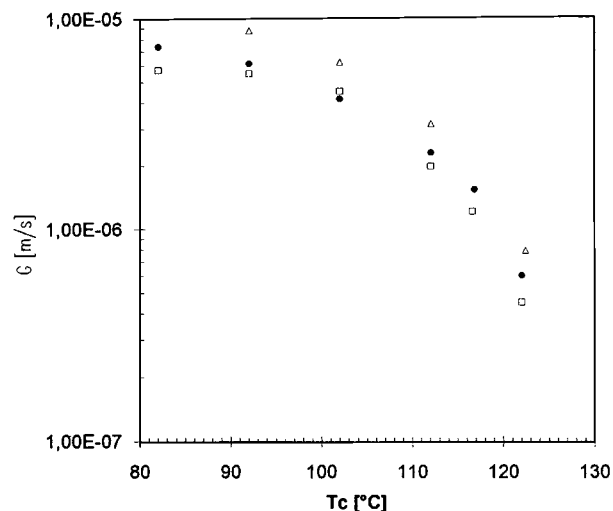


**Figure 8** Spherulitic growth speed as calculated from thin-film crystallization experiments at different crystallization temperatures for RE-type 5964/03 (□), HI-RE-type 7606/01 (△), and CR-type 5964/09 (●).

$$T_{c,n} - T_{c,u} \approx 15 \text{ K} \quad (2)$$

independent of the MFR. An earlier study by Avella et al.,<sup>35</sup> carried out on “Valtec” samples (RE grades) in a narrower range of  $M_w$ , showed a steady increase of the nucleation effect on the overall crystallinity with falling  $M_w$  thus, even amplifying the basic effect of the molar mass.

This development is also reflected in the mechanical properties of the nucleated materials. If one defines the relative increase in stiffness ( $E_F$ ) at a certain molar mass or MFR as

$$\Delta E_{\text{rel}}(\text{MFR}) = [E_{F,n}(\text{MFR})/E_{F,u}(\text{MFR})] - 1 \quad (3)$$

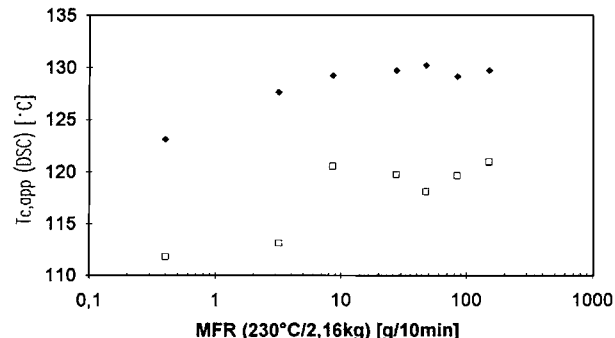


**Figure 9** Correlation between MFR (230°C/2.16 kg) and apparent crystallization temperature (DSC, cooling rate 10 K/min) for nonnucleated (□) and nucleated RE types (◆).

the effect mentioned before is expressed even stronger:  $\Delta E_{\text{rel}}$  rises up to an MFR of 50 g/10 min (corresponding to an  $M_w$  of 200 kg/mol) and falls again afterwards. The trend is the same for RE and CR grades, the maximum for the latter being in a lower MFR range, however (see Fig. 10). For the HI-RE grade,  $\Delta E_{\text{rel}}$  is at the same value as for the respective RE grade (0.44).

The mentioned trend inversion at a certain molar mass is repeated in case of the impact strength,  $a_N$ . As can be seen in Figure 11, the nucleation at higher  $M_w$  induces an embrittlement of the materials (rather expected from the higher stiffness values), while below an  $M_w$  range of 200 kg/mol even an increase of  $a_N$  is observed. The relation, which is shown here for RE grades, is practically the same for the CR grades. Generally, however, these differences must be considered critically because of the relation between the differences and the standard deviations in case of these rather brittle materials.

### Influence of Skin-Layer Formation

Obviously, a further effect adding to the simple crystallinity variation exists here. Evidence for that can be found in the light microscopy results of the cross-sections, which were investigated in parallel. Generally, a strong effect of the MFR on the spherulite size can be observed, but the formation of highly oriented skin layers, caused by shear-induced crystallization,<sup>36–40</sup> also changes significantly.

In the studies of Fujiyama et al.,<sup>36,37</sup> strong effects of  $M_w$  on both structural elements had been found: according to these results (which had been obtained on RE grades only), overall crystallinity increases with rising MFR, while the thickness of the skin layer ( $d_S$ ) decreases up to an MFR of 9 ( $M_w$  approx. 350), remaining constant then at a very low level.

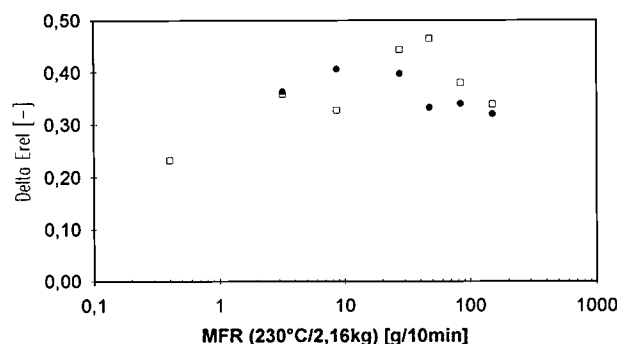


**Figure 10** Correlation between MFR (230°C/2.16 kg) and stiffness increase through nucleation ( $\Delta E_{\text{rel}}$ ) for RE (□) and CR types (●).

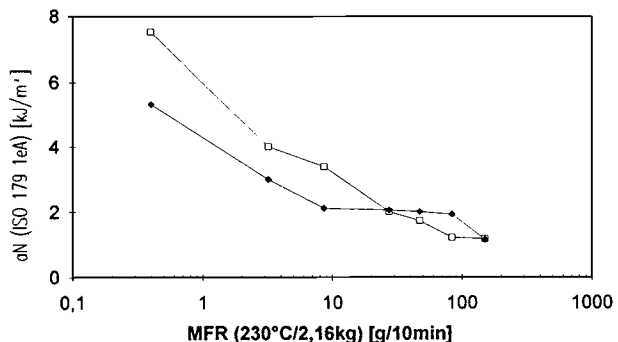


**Figure 11** Correlation between MFR (230°C/2.16 kg) and impact strength (ISO 179 1eA +23°C,  $a_N$ ) for non-nucleated (□) and nucleated RE types (◆).

The high orientation of this layer in the injection (c) direction was verified in x-ray scattering. Fujiyama successfully related the amount of orientation, and, subsequently,  $d_S$  to the relaxation time of the material, pointing out, however, that processing conditions (especially the melt temperature) have an even stronger effect on the final morphology.

Nucleation was found to influence both crystallinity and skin layer formation, resulting in higher values for overall crystallinity, orientation and  $d_S$ . Similar results were obtained by Jerschow<sup>39</sup> in model experiments (crystallization in a rectangular duct after short-time shearing) carried out to develop a theory of shear-induced crystallization.<sup>38,40</sup> In this case,  $d_S$  could be increased by a factor of 3 to 5 by heterogenous nucleation, depending on the MFR and the material type (RE or CR). The latter could not be fully explained by the differences in the rheology and flow profile, even though the theory of Janeschitz-Kriegl<sup>38</sup> gives a dependence of the intensity of shear-induced crystallization on  $\gamma'$ .<sup>4</sup>

From our previous investigations<sup>22</sup> two effects were already known: the spherulite-size decreases with rising MFR for both types of materials but is smaller for RE grades, and  $d_S$  decreases with rising MFR as well, being significantly lower in case of the CR grades. These facts were verified, concentrating on the skin layer (see Table III). The highly isotactic (HI-RE) grade shows two features appearing contradictory at first: a somewhat coarser spherulitic morphology in the core and a higher skin layer thickness. Taking into account the data from the crystallization experiments, this can be understood. While in the core, the combination of less nuclei (see Fig. 7) with higher spherulitic growth speed  $G$  (see Fig. 8) creates bigger spherulites, the shear-induced layer is extended by the higher value of  $G$ .

Nucleation changes the clearly spherulitic texture of the nonnucleated materials into a micro-crystalline morphology, which does not exhibit any visible differences over the whole range of materials. On the other hand, the skin layer is enhanced through nucleation. The thickness values measured in the MFR range between 3 and 50 g/10 min are summarized in Table III; again, a decrease in thickness with rising MFR also in case of the nucleated materials can be seen. A direct impression of the significant structural changes induced by the nucleation is given in Figure 12 for the case of the RE grade with MFR 8.6. The HI-RE material follows the changes in nucleation quite closely.

These effects show some interesting correlations to mechanics: both the "leveling" effect in  $E_F/M_w$  relation and the trend inversion in  $\Delta E_{\text{rel}}$  coincide with the disappearance of the skin layer, occurring for RE grades at  $\text{MFR} > 9$  and for nucleated RE grades at  $\text{MFR} > 50$ . If the high orientation of this skin layer is considered, which normally leads to unidirectional strengthening, the superior effect on the stiffness can be understood. The impact effects can be explained only if an inverse proportionality between crystallinity and  $a_N$  is assumed, corresponding to the fact that conventional impact modifiers are mostly amorphous. Details in this correlations must be sought for at a different structural level.

## CONCLUSIONS

The general correlation between crystallinity and mechanics of semicrystalline polymers is known from the literature.<sup>31</sup> As outlined above, the crystalline structure of a polymer is, under constant processing conditions, determined by the factors nucleation and spherulitic growth. In an expansion of earlier investigations<sup>22</sup> it could be shown that between two different types of PP-homopolymers (RE grades coming directly from the polymerization reactor and CR grades priorly subjected to a defined

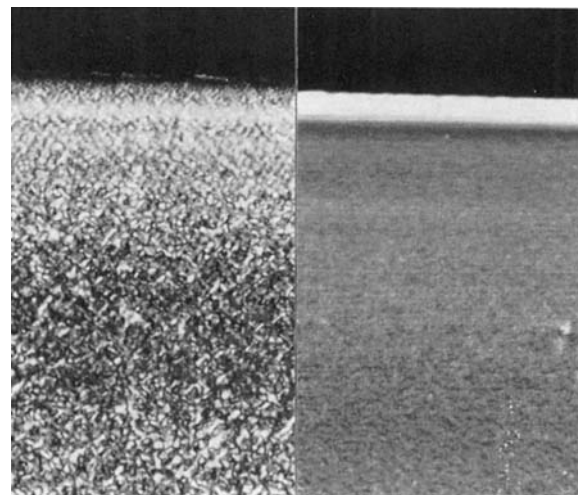


**Figure 12** Surface structure of specimen for mechanical testing showing the oriented skin layer for materials 5964/03 (RE type, not nucleated, left) and 5973/03 (RE type, nucleated, right); polarized light microscopy, enlargement 200 $\times$ .

degradation process) the main variation lies in the number of nuclei. If a material with higher isotacticity is compared to these, the main difference in properties results from a higher spherulitic growth speed.

The mechanical properties, however, are additionally influenced by the formation of highly oriented skin layers through shear-induced crystallization.<sup>38</sup> These structures are enhanced in case of higher  $M_w$  and, additionally, in case of higher isotacticity.

By adding heterogeneous nuclei in the form of nucleating agents the difference between RE and CR grades cannot be overcome. The nucleation effects appear to be similar for both categories, but are strongly dependent of the molar mass of the materials. In case of the highly isotactic material, the effects of nucleation and higher growth speed combine well to give optimized crystallinity and stiffness. The shear-induced skin structure is also significantly

**Table III** Effect of Molecular Structure and Nucleation on the Orientated Skin Layer in Injection-Molded Parts (Measured on Light Micrographs, Magnification 200 $\times$ )

Mat. No.	MFR [g/10 min]	$d_s$ (RE, base) [ $\mu\text{m}$ ]	$d_s$ (RE, nucl.) [ $\mu\text{m}$ ]	$d_s$ (CR, base) [ $\mu\text{m}$ ]	$d_s$ (CR, nucl.) [ $\mu\text{m}$ ]
02/08	3.2/3.4	10	20	5	17
03/09	8.6/8.6	7	15	0	12
04/10	27.5/28	5	10	0	10
05/11	47.3/51	0	10	0	15

influenced by the nucleating agent, causing an additional effect on mechanics. In any case, a correlation between the skin-layer formation ( $d_S(M_w)$ ) and the stiffness evolution ( $E_F(M_w)$ ) can be drawn. The situation is more complex in case of the impact properties, pointing to structural effects on a different scale.

The authors gratefully acknowledge the contribution of Ms. W. Pirgov, Mr. K. Keplinger, Mr. M. Königsdorfer, and Mr. J. Fiebig at PCD Polymere GmbH. Special thanks to Prof. H. Janeschitz-Kriegl for supervising the work at J. Kepler University Linz. Part of the work was supported by the Austrian "Forschungsfoerderungsfonds der gewerblichen Wirtschaft" under project No. 5/733.

## REFERENCES

1. W. Neißl and H. Ledwinka, *Kunststoffe*, **83**, 228–235 (1993).
2. E. Seiler, *Kunststoffe*, **85**, 1109–1116 (1995).
3. A. Zosel, *Rheol. Acta*, **10**, 215–220 (1971).
4. A. Schausberger, *Rheol. Acta*, **25**, 596–608 (1986).
5. C. A. Hieber and H. H. Chiang, *Rheol. Acta*, **28**, 321–328 (1989).
6. S. H. Wasserman and W. W. Graessley, *J. Rheol.*, **36**, 543–572 (1992).
7. T. Ogawa, *J. Appl. Polym. Sci.*, **44**, 1869–171 (1992).
8. R. Greco and G. Ragosta, *J. Mater. Sci.*, **23**, 4171–4180 (1988).
9. D. Tartari and M. Bramuzzo, *Kunststoffe*, **83**, 460–467 (1993).
10. R. Zhang, H. Zhang, X. Lou, and D. Ma, *J. Appl. Polym. Sci.*, **51**, 51–56 (1994).
11. D. W. van Krevelen and P. J. Hoflyzer, *Properties of Polymers*, Elsevier Scientific, Amsterdam, 1975.
12. F. L. Binsbergen, *Polymer*, **11**, 253–259 (1970).
13. T. S. Dziedzianowicz and W. W. Cox, *SPE ANTEC*, 540–545 (1985).
14. G. Hebert, *SPE ANTEC*, 579–586 (1994).
15. S. Z. D. Cheng, J. J. Janimak, A. Zhang, and E. T. Hsieh, *Polymer*, **32**, 648–655 (1991).
16. J. J. Janimak, S. Z. D. Cheng, P. A. Giusti, and E. T. Hsieh, *Macromolecules*, **24**, 2253–2260 (1991).
17. J. J. Janimak, S. Z. D. Cheng, A. Zhang, and E. T. Hsieh, *Polymer*, **33**, 728–735 (1992).
18. R. Phillips, G. Herbert, J. News, and M. Wolkowicz, *Polym. Eng. Sci.*, **34**, 1731–1743 (1994).
19. see, e.g., EP 255.693 for Chisso Corp.
20. A. Zambelli, P. Locatelli, M. C. Sacchi, and I. Trotto, *Macromolecules*, **6**, 925–926 (1973).
21. H.-L. Chen and J. C. Hwang, *Polymer*, **36**, 4355–4357 (1995).
22. M. Gahleitner, K. Bernreitner, W. Neißl, C. Paulik, and E. Ratajski, *Polym. Testing*, **14**, 173–178 (1995).
23. G. Eder, H. Janeschitz-Kriegl, and S. Liedauer, *Prog. Polym. Sci.*, **15**, 629–714 (1990).
24. H. Janeschitz-Kriegl, H. Wippel, C. Paulik, and G. Eder, *Coll. Polym. Sci.*, **271**, 1107–1115 (1993).
25. E. Ratajski and H. Janeschitz-Kriegl, *Coll. Polym. Sci.*, to appear.
26. J. Brandrup and E. M. Immergut, Eds., *Polymer Handbook*, Interscience, New York, 1989.
27. R. Greco and G. Ragosta, *Plastics Rubber Proc. Appl.*, **7**, 163–171 (1987).
28. K. Friedrich, *Kunststoffe*, **69**, 796–801 (1979).
29. J. L. Way, J. R. Atkinson, and J. Nutting, *J. Mater. Sci.*, **9**, 293–299 (1974).
30. A. O. Ibhodon, *J. Appl. Polym. Sci.*, **46**, 2123–2139 (1992).
31. J. K. Halpin and J. L. Kardos, *J. Appl. Phys.*, **43**, 2235–2240 (1972).
32. M. R. Dichman, *SPE ANTEC*, 483–487, 1994.
33. B. Fillon, B. Lotz, A. Thierry, and J. C. Wittmann, *J. Polym. Sci. B: Polym. Phys.*, **31**, 1395–1405 (1993).
34. H. N. Beck, *J. Appl. Polym. Sci.*, **11**, 673–685 (1967).
35. M. Avella, R. dell'Erba, E. Martuscelli, and G. Ragosta, *Polymer*, **34**, 2951–2960 (1993).
36. M. Fujiyama, in *Polypropylene*, Vol. 1, J. Karger-Kocsis, Ed., Chapman & Hall, London 1995, pp. 167–204.
37. M. Fujiyama and T. Wakino, *J. Appl. Polym. Sci.*, **43**, 57–81 (1991).
38. S. Liedauer, G. Eder, H. Janeschitz-Kriegl, P. Jerschow, W. Geymayer, and E. Ingolic, *Int. Pol. Proc.*, **8**, 236–244 (1993).
39. P. Jerschow, PhD Thesis, Linz, 1994.
40. S. Liedauer, G. Eder, and H. Janeschitz-Kriegl, *Int. Polym. Proc.*, **10**, 243–250 (1995).

Received November 30, 1995

Accepted February 22, 1996